

2-1-2014

## The Creation of 360° Domain Walls in Ferromagnetic Nanorings by Circular Applied Magnetic Fields

Jessica E. Bickel  
*Cleveland State University*, [j.e.bickel@csuohio.edu](mailto:j.e.bickel@csuohio.edu)

Spencer A. Smith  
*Mount Holyoke College*

Katherine E. Aidala  
*Mount Holyoke College*, [kaidala@mtholyoke.edu](mailto:kaidala@mtholyoke.edu)

Follow this and additional works at: [https://engagedscholarship.csuohio.edu/sciphysics\\_facpub](https://engagedscholarship.csuohio.edu/sciphysics_facpub)

 Part of the [Physics Commons](#)

[How does access to this work benefit you? Let us know!](#)

---

### Repository Citation

Bickel, Jessica E.; Smith, Spencer A.; and Aidala, Katherine E., "The Creation of 360° Domain Walls in Ferromagnetic Nanorings by Circular Applied Magnetic Fields" (2014). *Physics Faculty Publications*. 192.  
[https://engagedscholarship.csuohio.edu/sciphysics\\_facpub/192](https://engagedscholarship.csuohio.edu/sciphysics_facpub/192)

This Article is brought to you for free and open access by the Physics Department at EngagedScholarship@CSU. It has been accepted for inclusion in Physics Faculty Publications by an authorized administrator of EngagedScholarship@CSU. For more information, please contact [library.es@csuohio.edu](mailto:library.es@csuohio.edu).

# The creation of 360° domain walls in ferromagnetic nanorings by circular applied magnetic fields

Jessica E. Bickel,<sup>a)</sup> Spencer A. Smith, and Katherine E. Aidala<sup>b)</sup>  
*Department of Physics, Mount Holyoke College, South Hadley, Massachusetts 01075, USA*

(Presented 5 November 2013; received 23 September 2013; accepted 5 November 2013; published online 18 February 2014)

Switching behavior in ferromagnetic nanostructures is often determined by the formation and annihilation of domain walls (DWs). In contrast to the more familiar 180° DWs found in most nanostructures, 360° DWs are the proposed transition state of nanorings. This paper examines the formation of 360° DWs created by the application of a circular magnetic field using micromagnetic simulations. 360° DWs form from pairs of canting moments that are oppositely aligned, which each grow to form rotated domains bounded by two 180° DWs and the 180° DWs combine to form 360° DWs. The resulting 360° DWs occur in pairs of opposite topological winding number due to these domains of opposite canting direction. The final number of DWs formed is greatly impacted by symmetry, both of the ring and of the placement of the circular magnetic field. © 2014 AIP Publishing LLC. [<http://dx.doi.org/10.1063/1.4864441>]

The competition between exchange, magnetostatic, and Zeeman energies in ferromagnetic nanorings (FMNRs) and nanostructures can result in intriguing physical states. These energetic balances control the formation and annihilation of domain walls (DWs) that typically determine the switching behavior in magnetic nanostructures, some of which are proposed as potential magnetoresistive random-access memory devices.<sup>1,2</sup> Racetrack memory proposals<sup>1</sup> use the DW to separate magnetic bits, motivating work to understand the shape, energies, and injection of 180° DWs into magnetic wires.<sup>3,4</sup> Less work has been done to examine 360° DWs. 360° DWs, which are a combination of two 180° DWs with the same topological winding direction, have been predicted as the transition state of thin ferromagnetic nanorings switching between a clockwise (CW) and counterclockwise (CCW) vortex state under an applied circular magnetic field.<sup>5</sup> Such fields have only recently become of interest to experimental<sup>6,7</sup> and computational studies.<sup>5,8,9</sup> Recent studies of 360° DWs have examined DW annihilation,<sup>5,10</sup> DW formation in a 1D case with a radially uniform field,<sup>11,12</sup> and DW formation controlled by the placement of anti-notches as nucleation sites.<sup>9</sup> Here, we investigate how 360° DWs nucleate and form in a symmetric ring under a radially decaying azimuthal magnetic field in order to better understand 360° DWs and their topological constraints and to inform future experiments on ferromagnetic nanorings.

Calculations were performed using OOMMF,<sup>13</sup> which iteratively solves the Landau-Lifshitz-Gilbert equation. The simulations were performed for permalloy using a saturation magnetization of  $M_s = 8.6 \times 10^5$  A/m, a six-nearest neighbor exchange parameter of  $A = 1.3 \times 10^{-13}$  J/m, and no crystal-line anisotropy. The calculations were performed at  $T = 0$  K in order to clearly see the formation mechanisms of 360°

DWs. Previous studies have shown such walls are metastable at room temperature<sup>5,10,14</sup> and therefore accessible and of interest to experimental studies. The rings studied here have an outer diameter (OD) of 800 nm, an inner diameter (ID) of 200 nm and a thickness of 5 nm with a grid of  $3.2 \times 3.2 \times 5$  nm<sup>3</sup>/cell. No qualitative changes in switching behavior occurred when changing the inner diameter of the ring or changing the shape to an elliptical hole. The applied circular magnetic field varies as a function of position according to the equation for the magnetic field created by current in an infinite wire such that  $B \propto \frac{I}{R}$ , where  $I$  is the applied current and  $R$  is the distance from the wire. The applied current was placed either at the exact center of the ring or slightly off center to investigate the effects of symmetry.

The magnetic configuration that minimizes both the exchange and magnetostatic energies in these rings is a vortex state with the moments aligned in a CW (Fig. 1(c)) or CCW (Fig. 1(b)) direction, which both have a topological winding number of  $\pm 1$ . It is helpful to also define the vorticity,<sup>5</sup>  $V \propto (\hat{r} \times \vec{M})$ , where  $\hat{r}$  is the radial unit vector and  $\vec{M}$  is the magnetization direction; Therefore, CCW (CW) has a vorticity of  $+1$  ( $-1$ ). Figure 1(a) shows the hysteresis curve of a ring in a circular field, plotting vorticity vs. applied current. Under strong negative fields, the ring is a perfect CW vortex as in Fig. 1(c). As the field is reduced and reversed, the ring passes through the transition state shown in Fig. 1(d), where most of the magnetic moments have rotated to align with the applied field. However, this rotation creates two 360° DWs. The DWs rotate in opposite directions relative to the underlying vortex, as can be seen by the schematics in Fig. 1(d) and thus have opposite topological winding numbers,  $\Omega$ . The winding numbers are defined such that  $+1$  ( $-1$ ) indicates the DW rotates in the same (opposite) direction as the underlying vortex. As the magnetic field is increased, first the  $\Omega = +1$  DW and then the  $\Omega = -1$  DW annihilate, in agreement with previous work.<sup>5,9,10</sup> When both DWs annihilate,

<sup>a)</sup>Electronic mail: jebickel@mholyoke.edu.

<sup>b)</sup>Electronic mail: kaidalala@mholyoke.edu.

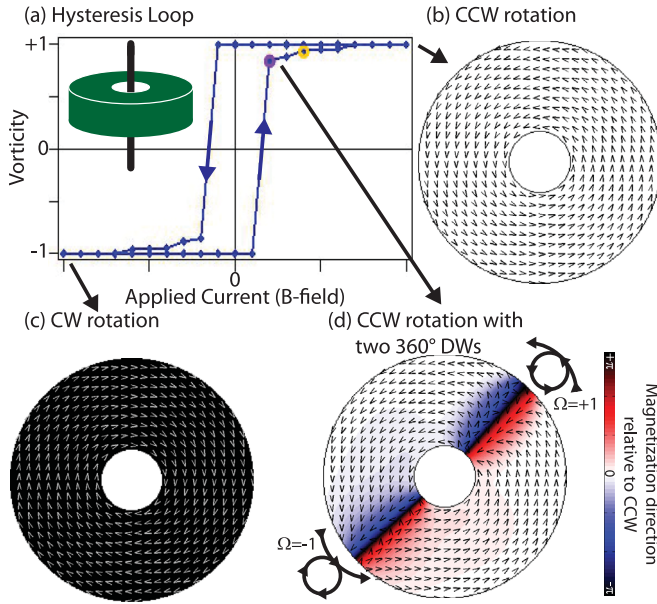


FIG. 1. (a) Hysteresis loop for a ferromagnetic nanoring transitioning between (b) counterclockwise and (c) clockwise vortex states. A circular magnetic field is applied by passing current through the ring center, as shown schematically in the inset. While switching between the CCW and CW ground states, the ring passes through an intermediate state that has two  $360^\circ$  domain walls (d). Color scale: white = CCW, black = CW, red = rotation inward, and blue = rotation outward.

the result is a perfect CCW vortex, shown in Fig. 1(b). The hysteresis loop in Fig. 1(a) is for a current applied at  $r = 2.3$  nm from the center the ring. The significance of this offset will be discussed later.

To examine the formation of  $360^\circ$  DWs, we focused on the point just after the jump in the hysteresis loop, indicated by the purple circle in Fig. 1(a). Figures 2(a)–2(c) show snapshots of the magnetic structure of the ring at different stages of DW formation induced by an applied current of  $I = -60$  mA at the center of the nanoring. The arrowheads show the magnetization direction, and the color scale shows the degree and direction of rotation away from the original CCW vortex with red (blue) indicating a rotation inward (outward) toward the center (edge) of the ring. The beginning of the reversal is shown in Fig. 2(a) where small regions of nanoring are red (blue) as the magnetic moments begin to cant slightly inward (outward). The magnified region more clearly shows this initial canting. The canting occurs near the inner edge of the nanoring because the magnetic field is strongest there, but not exactly at the inner edge due to magnetostatic considerations. The top of Fig. 2(d) is a schematic of a 1-dimensional (1D) cut through the magnified region and shows the spin canting inward (down). The lower slice shows an initial outward canting; the energy of these two canting directions is degenerate. Adjacent domains always cant in opposite directions for two reasons. If two adjacent domains canted in the same direction, they would simply merge to form one larger domain. Also, canting in opposite directions lowers the magnetostatic energy relative to canting in the same direction.

After the initial canting, the rotated moments continue to reverse direction, and adjacent moments begin to rotate, influenced by both the magnetic field and the exchange field from their rotated neighbors. The resulting magnetic

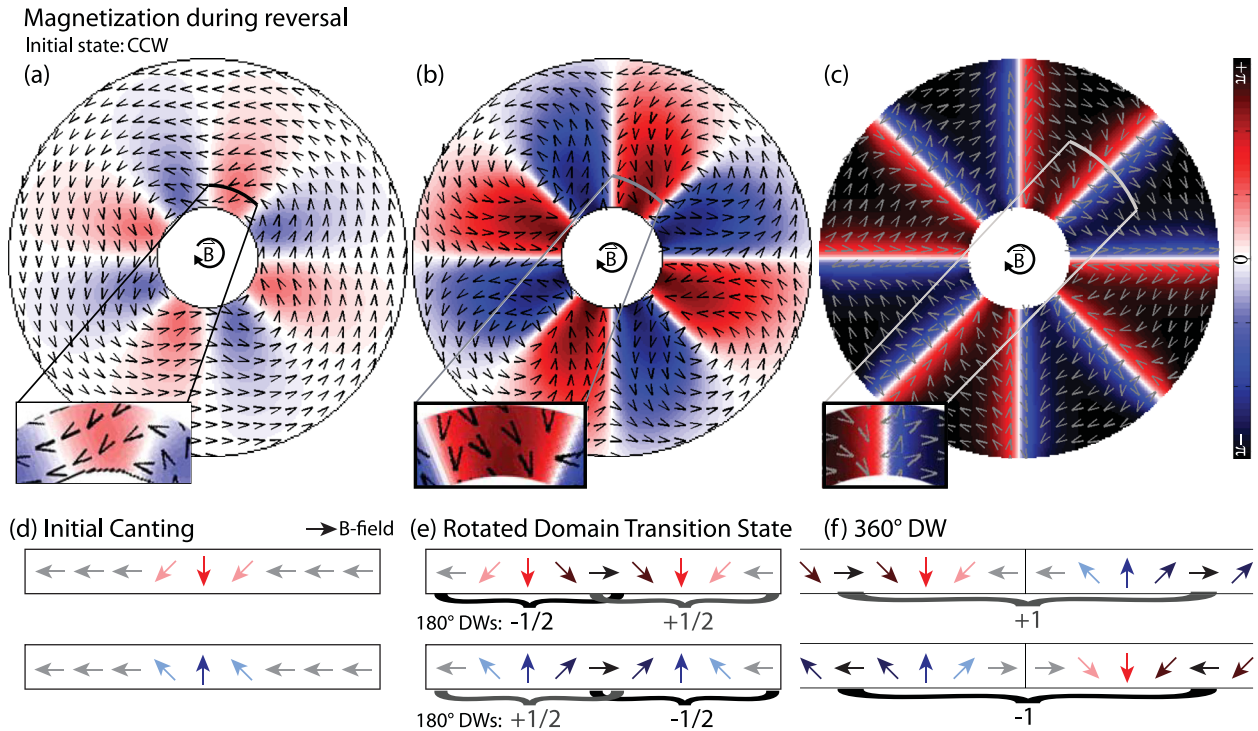


FIG. 2. (a)–(c) Snapshots of the magnetization state during reversal of a ring with  $I = -60$  mA applied at the exact center of the ring. The color scale shows the degree of canting of a small region of magnetic moments from a perfect CCW rotation, with red canting inward toward the center, blue canting outward towards the edge, and black being fully reversed to the CW rotation. Magnetic reversal in these rings occurs with an initial canting of the magnetization (left) as shown schematically in (d). The magnetic moments continue to rotate forming domains bounded by two  $180^\circ$  DWs (e). As the rotation continues to completely reverse,  $180^\circ$  DWs from adjacent rotated domains converge to form  $360^\circ$  DWs (f).

structure is shown in Fig. 2(b). The inset shows that the center of the region is close to being completely reversed. A 1D schematic of the region with the central spin completely reversed is shown in Fig. 2(e). When the central spin, the first moment to cant, has reversed direction by rotating a full  $180^\circ$ , the result is two  $180^\circ$  DWs of opposite winding number, one CW ( $\Omega = +\frac{1}{2}$ ) and one CCW ( $\Omega = -\frac{1}{2}$ ), where  $\Omega$  is measured relative to the CW vortex. The resulting structure has been predicted by a 1D model as the transition for nanorings of sufficiently large outer diameters and widths and has previously been termed an instanton.<sup>11,12</sup> The canting of magnetic spins begins close to the inner edge of the ring and spreads both angularly and radially around the nanoring. Until the spins at the outer edge are reversed, the transition structure is not stable and will unwind to the initial CCW rotation if the magnetic field is removed, as happens when any field less than  $I_c$ , the critical current for reversal for that size of nanoring.

Each of the rotated magnetic domains is bounded on either side by two  $180^\circ$  DWs of opposite winding number, as shown in Fig. 2(e). As the domain center expands due to its alignment with the applied field, the  $180^\circ$  DWs move apart until they encounter those of adjacent rotated domains. These two converging  $180^\circ$  DWs always have the same winding number for symmetry reasons as seen in Fig. 2(f), which combines the two rotated transition structures of Fig. 2(e) to form both  $\Omega = +1$  and  $\Omega = -1$   $360^\circ$  DWs. Thus,  $360^\circ$  DWs are formed at the boundaries between the canting regions and alternate winding numbers positive and negative around the ring and one pair of  $+1/-1$  DWs is formed for each pair of rotated domains. This work is in agreement with previous work on rings with two anti-notches.<sup>9</sup> The anti-notches act as nucleation points for the initial canting and the two oppositely canted domains result in a pair of  $360^\circ$  DWs.

Symmetry can significantly affect the nucleation and growth of the canting domains. The ring described in Fig. 2 is perfectly symmetric and resulted in eight DWs. For the ring shown in Fig. 1, the symmetry was broken by applying the current at  $r = 2.3$  nm from the center of the ring. Four canting domains were formed; however, those closest to the applied current experienced a higher Zeeman field and thus grew faster, at the expense of the domains farther from the field that were destroyed before they were fully formed. More generally, in a symmetric ring, the asymmetric placement of the current will always result in a single pair of  $360^\circ$

DWs. In a more extreme case of asymmetry, a ring with an off-center elliptic hole can lead to no stable DWs due to the effects of the canting nucleation and growth and the energetic requirement that DWs minimize their length. Even a small asymmetry in the simulation, deleting a single  $3.2 \times 3.2$  nm magnetic cell, can affect the formation of DWs. This is in agreement with previous work that showed that imposing a square grid on a round structure can create local regions of magnetic charge that act as nucleation points for reversal and affect the number of DWs created.<sup>9</sup> These symmetric considerations mean that it may be possible to direct the location of  $360^\circ$  DWs by adjusting the ring shape and placement of the current, but experimental realities of defects and pinning sites make this unlikely to be realized. More importantly, when considering the experimental difficulty of applying the current symmetrically with sub-nanometer precision, this work suggests that at least one pair, and most likely only a single pair, of  $360^\circ$  DWs will be experimentally obtainable.

This work was supported by NSF Grant No. DMR-1207924. The simulations were performed at the Center for Nanoscale Systems (CNS) computational facilities at Harvard University, a member of the National Nanotechnology Infrastructure Network (NNIN), which is supported by NSF Award No. ECS-0335765.

- <sup>1</sup>S. S. P. Parkin, M. Hayashi, and L. Thomas, *Science* **320**, 190 (2008).
- <sup>2</sup>J.-G. Zhu, Y. Zheng, and G. A. Prinz, *J. Appl. Phys.* **87**, 6668 (2000).
- <sup>3</sup>M. Hayashi, L. Thomas, C. Rettner, R. Moriya, and S. S. P. Parkin, *Nat. Phys.* **3**, 21 (2007).
- <sup>4</sup>A. Kunz and S. C. Reiff, *Appl. Phys. Lett.* **94**, 192504 (2009).
- <sup>5</sup>A. Goldman, A. S. Licht, Y. Sun, Y. Li, N. R. Pradhan, T. Yang, M. T. Tuominen, and K. E. Aidala, *J. Appl. Phys.* **111**, 07D113 (2012).
- <sup>6</sup>N. R. Pradhan, A. S. Licht, Y. Li, Y. Sun, M. T. Tuominen, and K. Aidala, *Nanotechnology* **22**, 485705 (2011).
- <sup>7</sup>T. Yang, N. R. Pradhan, A. Goldman, M. Kemei, A. Licht, Y. Li, M. T. Tuominen, and K. E. Aidala, *Appl. Phys. Lett.* **98**, 242505 (2011).
- <sup>8</sup>M. Maicas, *Physica B* **343**, 247 (2004).
- <sup>9</sup>A. L. G. Oyarce, T. Trypiniotis, P. E. Roy, and C. H. W. Barnes, *Phys. Rev. B* **87**, 174408 (2013).
- <sup>10</sup>G. D. Chaves-O'Flynn, D. Bedau, E. Vanden-Eijnden, A. D. Kent, and D. L. Stein, *IEEE Trans. Magn.* **46**, 2272 (2010).
- <sup>11</sup>K. Martens, D. L. Stein, and A. D. Kent, *Phys. Rev. B* **73**, 054413 (2006).
- <sup>12</sup>G. D. Chaves-O'Flynn, A. D. Kent, and D. L. Stein, *Phys. Rev. B* **79**, 184421 (2009).
- <sup>13</sup>M. Donahue and D. Porter, *OOMMF User's Guide, Version 1.0* (Nist, Gaithersburg, MD, 1999).
- <sup>14</sup>C. B. Muratov and V. Osipov, *IEEE Trans. Magn.* **45**, 3207 (2009).

Journal of Applied Physics is copyrighted by the American Institute of Physics (AIP). Redistribution of journal material is subject to the AIP online journal license and/or AIP copyright. For more information, see <http://ojps.aip.org/japo/japcr/jsp>

Journal of Applied Physics is copyrighted by the American Institute of Physics (AIP).  
Redistribution of journal material is subject to the AIP online journal license and/or AIP  
copyright. For more information, see <http://ojps.aip.org/japo/japcr/jsp>